

# Concept and Demonstration of Individual Probe Actuation in Two-Dimensional Parallel Atomic Force Microscope System

Terunobu AKIYAMA<sup>1\*</sup>, Laure AESCHIMANN<sup>1</sup>, Laura CHANTADA<sup>2</sup>, Nico. F. DE ROOIJ<sup>1</sup>, Harry HEINZELMANN<sup>4</sup>, Hans P. HERZIG<sup>3</sup>, Omar MANZARDO<sup>3</sup>, André MEISTER<sup>4</sup>, Jérôme POLESEL-MARIS<sup>4</sup>, Raphaël PUGIN<sup>4</sup>, Urs STAUFER<sup>1</sup>, and Peter VETTIGER<sup>1,4</sup>

<sup>1</sup>SAMLAB, Institute of Microtechnology, University of Neuchâtel, Jaquet-Droz 1, 2002 Neuchâtel, Switzerland

<sup>2</sup>University of Santiago de Compostela, Santiago de Compostela, Spain

<sup>3</sup>OPTICS, Institute of Microtechnology, University of Neuchâtel, A.-L. Breguet 2, 2000 Neuchâtel, Switzerland

<sup>4</sup>Swiss Center for Electronics and Microtechnology CSEM SA, Jaquet-Droz 1, 2002 Neuchâtel, Switzerland

A concept of an array actuator that is used to control the tip-sample separation of cantilevers in a two-dimensional (2D) probe array scanning system is proposed in this article. The feasibility of the concept is demonstrated with a  $10 \times 10$  array actuator with  $500 \mu\text{m}$   $xy$ -pitches. The array actuator is made by slicing a bulk piezoceramic block. The obtained maximum actuation of a single probe was  $2.19 \mu\text{m}_{\text{p-p}}$  at  $\pm 168 \text{V}_{\text{p-p}}$ . A major issue for the actuator was the insufficient strength of the frame of the probe array chip. The demonstrated array actuator is highly compatible with previously developed parallel readout modules that use either a parallel optical beam or integrated piezoresistive deflection sensing. A large-scale 2D probe array is our ultimate target.

KEYWORDS: SPM, AFM, probe array, actuator, optical heterodyne interferometry

## 1. Introduction

Scanning probe technologies are currently the most popularly used tools in nanoscience and technology research for nanoscale imaging, spectroscopy, modification, and manipulation. However, one of the major limitations of today's scanning probe instruments is the relatively small field of view. Nanometer scale resolution can only be achieved over narrow scan ranges, hence the overall throughput of such probe instruments is very limited. The availability and operation of one- or two-dimensional (1D or 2D) probe arrays will address the field of view and throughput limitations of current single-probe systems and instruments. The parallel operation of large probe arrays can be used to increase sensing area and throughput without sacrificing individual sensor sensitivity.<sup>1,2)</sup> Major technological challenges for implementing large probe arrays are the parallel readout of cantilever deflection and the individual actuations of each cantilever. Sensors and actuators that are often used in probe arrays are briefly summarized elsewhere.<sup>3)</sup>

Our goal is to develop a large-scale 2D probe array for applications to research in life sciences, e.g., biological and medical experiments, that requires probe operation in liquids. For imaging "soft" samples, it is important to precisely control the loading force applied to the sample. Actuators for regulating the tip-sample distance of each probe are indispensable in such a 2D probe array system. To date, we have studied two different approaches to the parallel readout of cantilevers in a 2D probe array system. One is the use of an integrated piezoresistive sensor<sup>4,5)</sup> and the other is the use of an optical parallel beam readout based on heterodyne interferometry.<sup>6,7)</sup> In the same frame work, we developed an actuation module, which is an array actuator to individually control the tip-sample separation of each cantilever. The concept and performance of the first demonstrator of the actuation module are described in this article.

## 2. Probe Actuation in Arrays

### 2.1 Concept

The essential design criterion for actuation modules in definition is a good compatibility with two different detection modules, i.e., the integrated piezoresistive sensor and parallel beam readout. The actuation modules to be developed can be integrated either on each cantilever or on the system side. Since the tip is worn off by scanning samples and should be replaced often, we prefer to integrate as many necessary functionalities as possible on the system side, not on the cantilever chip in order to make the array chip inexpensive and disposable. In addition, if a simple 2D probe array chip with no integrated functionalities can be employed and the need to connect wires to the chip can be eliminated, the changing of the chip can be made simple and easy. Furthermore, the modules on the system side can be well isolated from the medium surrounding the probe array, e.g., liquid and gas. For these reasons, we decided to investigate the external actuation principle. It is preferred that the demonstrator is capable of parallel imaging of biological samples in a liquid environment.

Figure 1(a) shows the concept of the probe array system using parallel optical beam cantilever deflection detection. For the simple fabrication of a cantilever array, the optical approach has been chosen for the actuator demonstrator. However, this approach can equally be applied to the concept of a self-sensing cantilever, such as piezoresistive detection. The optical beam array is focused on each cantilever using microlens array. The cantilevers are mechanically connected to a rigid frame with an elastic hinge which is much stiffer than cantilever. For the control of tip-sample separation, the elastic hinge is bent by an external actuator. Figure 1(b) shows the concept of the external actuation approach. A small block of piezoceramic is employed to yield a displacement and a glass bead transfers the actuation to the hinge. Since only one end of the hinge is fixed and the cantilever is at the other end, the output displacement of the piezoceramic is mechanically

\*E-mail address: terunobu.akiyama@unine.ch

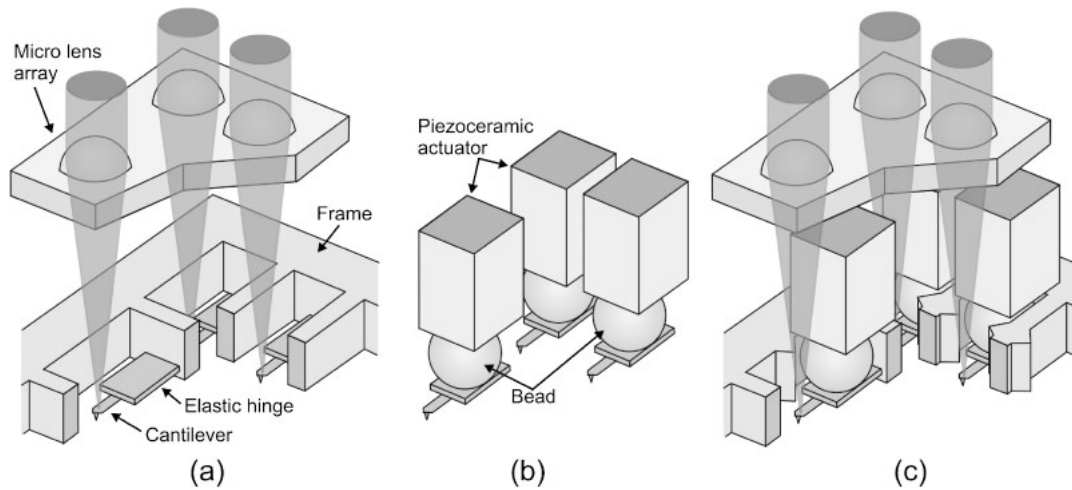


Fig. 1. (a) Parallel beam cantilever deflection system with heterodyne detection,<sup>6,7</sup> (b) concept of external actuation, and (c) targeting parallel probe AFM apparatus.

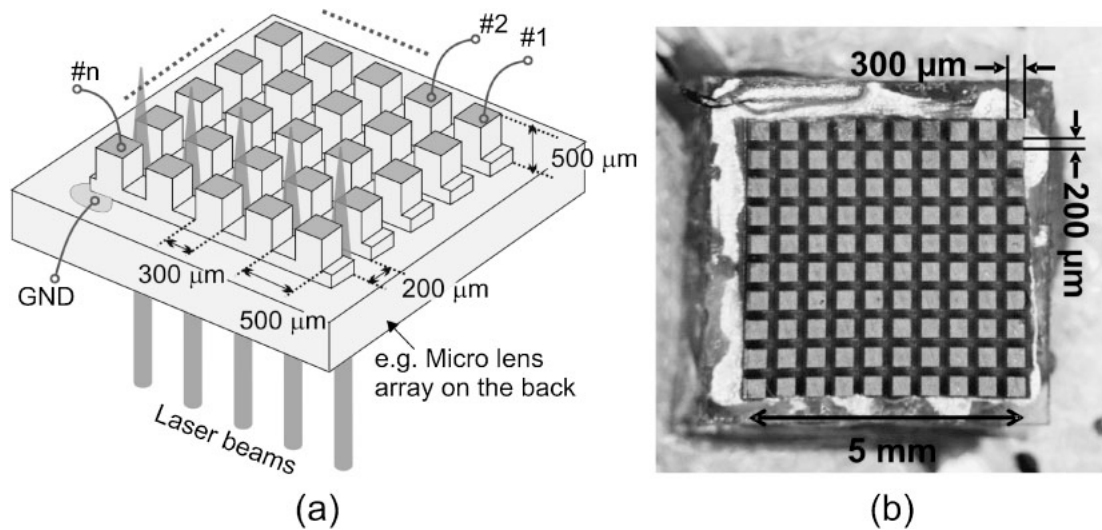


Fig. 2. (a) Piezoceramic block (array actuator) glued to back surface of the microlens array chip. (b) Fabricated  $10 \times 10$  array actuator.

amplified at the tip of the sensing cantilever. Both piezoceramic block and bead have to be small enough so that they can be well incorporated in a space for one cantilever [Fig. 1(c)]. In the case of the integrated piezoresistive sensing system, the space issue can be much relaxed.

## 2.2 Design and fabrication

Figure 2 shows the design of the array actuator based on a piezoceramic (PZT) block. The piezoceramic block is glued to a glass plate, which can also include a microlens array chip in the case of optical beam deflection detection. The block is fabricated by slicing a bulk piezoceramic plate into a matrix using a standard dicing saw for semiconductors. In one direction, the full thickness of the piezoceramic plate is cut, whereas only a certain depth is cut in the other direction. In Fig. 2(a), five sections are connected to form a row and the rows are completely separated. This configuration provides space for optical beams to reach the cantilever. An actual  $10 \times 10$  piezoceramic block is shown in Fig. 2(b). The rows are not fully separated, i.e., only a certain depth is cut in both directions, to facilitate the handling of the piezoceramic chip. The thickness of the piezoceramic plate

is  $500 \mu\text{m}$ . There are metal layers on both sides when purchased. For dicing convenience, the pitch of one section is fixed to  $500 \mu\text{m}$ , with  $300 \mu\text{m}$  for actuation and  $200 \mu\text{m}$  for separation (Fig. 2) in both  $xy$ -directions. The sliced depth is  $400 \mu\text{m}$ , leaving  $100 \mu\text{m}$ . After slicing, the piezoceramic chip is glued on a plane glass plate with conductive epoxy. This terminal is grounded for operation.

To individually address and drive each piezoceramic block, electrical connections have to be established from external driving sources to each block. For this purpose, a polyester film called Mylar<sup>®</sup> with embedded metal lines is employed. Mylar film has superior strength, high heat resistance, and excellent insulating properties. In addition, it is basically transparent, allowing laser beams to pass through it. Figure 3 shows a schematic of the targeting probe array setup with the parallel beam detection system. Each metal line on the Mylar film has a small pad at one end to connect the piezoceramic block and a large pad at the other end to connect a macropad to a printed circuit board (PCB). The small pad is simply pressed onto the metal electrode of the piezoceramic block to establish electrical connection upon assembly of the whole setup. Since Mylar is a good

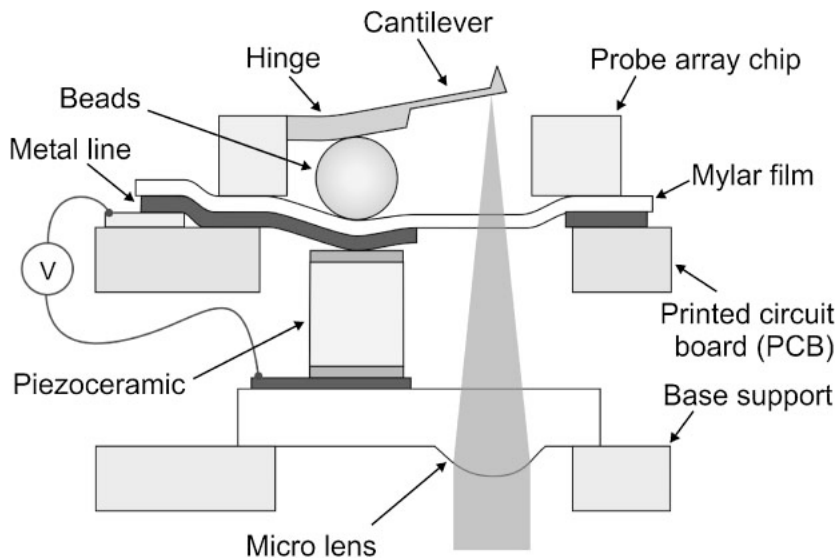


Fig. 3. Cross-section of targeting AFM with piezoceramic block actuator and parallel beam cantilever deflection detection system [cf. Fig. 1(c)]. The microlens and optical passes on the actuator chip are not realized in the actual demonstrator.

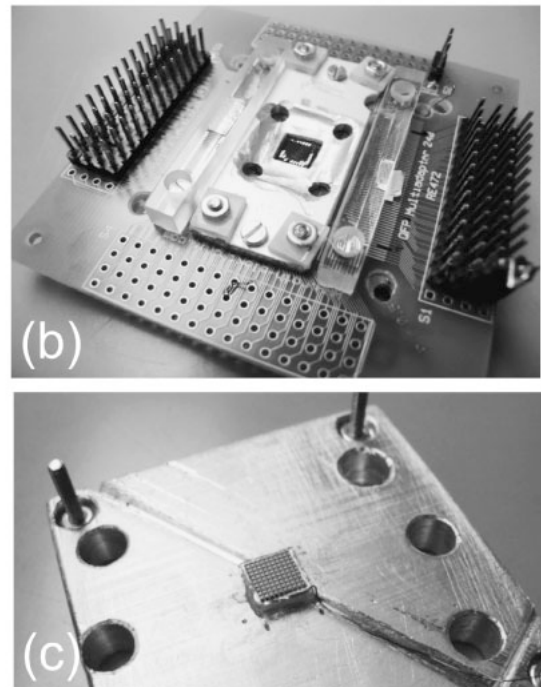
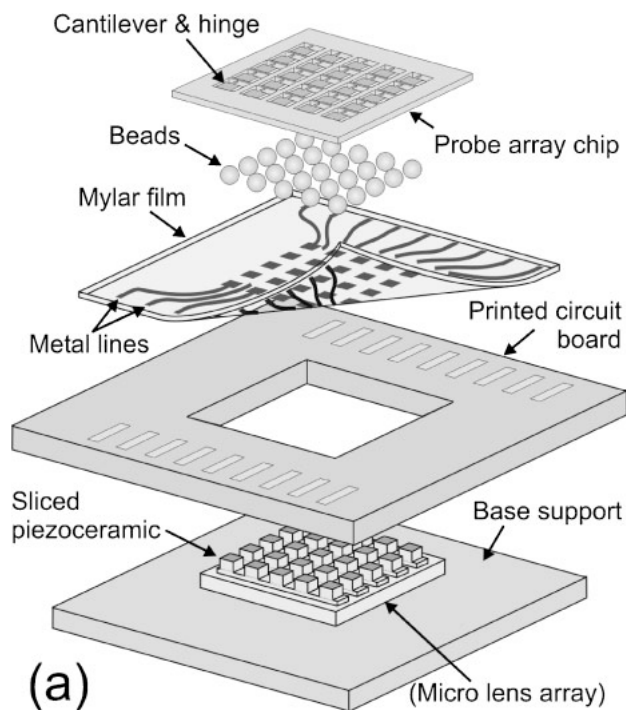


Fig. 4. (a) Major components of probe actuation demonstrator, (b) photograph of assembled demonstrator, and (c) base support with sliced piezoceramic chip.

insulator, the cantilever chip can be electrically isolated from any high-voltage signal to drive the piezoceramic blocks. Furthermore, the use of Mylar film potentially allows us to perform parallel atomic force microscopy (AFM) imaging in a liquid environment. Mylar film protects the array of actuators from liquid when the cantilever chip is completely immersed in a liquid solution. In an actual setup, a 12- $\mu\text{m}$ -thick Mylar film was used. The electrodes are made of a 1- $\mu\text{m}$ -thick aluminum film, which was evaporated and patterned for the pads and connecting lines by standard photolithography and wet etching.

Figure 4(a) shows the major components of the probe actuation demonstrator: from top, probe array chip, beads, Mylar film with Al electrodes on its back surface, PCB, an array of piezoceramic block, a plane glass chip instead of a microlens array, and a rigid substrate. Figure 4(b) shows a

photograph of the assembled demonstrator of a  $10 \times 10$  probe array with  $500 \mu\text{m}$  pitches, and Fig. 4(c) shows the base support with a piezoceramic actuator. The thickness of the cantilever chip is set at  $265 \mu\text{m}$  to enable the use beads of  $300 \mu\text{m}$  diameter. The beads are actually sold as sapphire ball lens by Swiss Jewel. The probe array chip was fabricated only to demonstrate the actuator concept, and its design was simplified, i.e., no tips and uniform thickness of the cantilever and hinge parts. There were three major fabrication steps: (1) forming of the cantilever and hinge by KOH etching, (2) deep reactive ion etching (DRIE) from the back surface of the wafer, and (3) thermal oxidation and oxide etching in BHF to remove silicon debris.

The assembly of the demonstrator was carried out as follows: Two edges of the Mylar film, where large pads were delineated, were fixed on the PCB by two acrylic bars [cf.

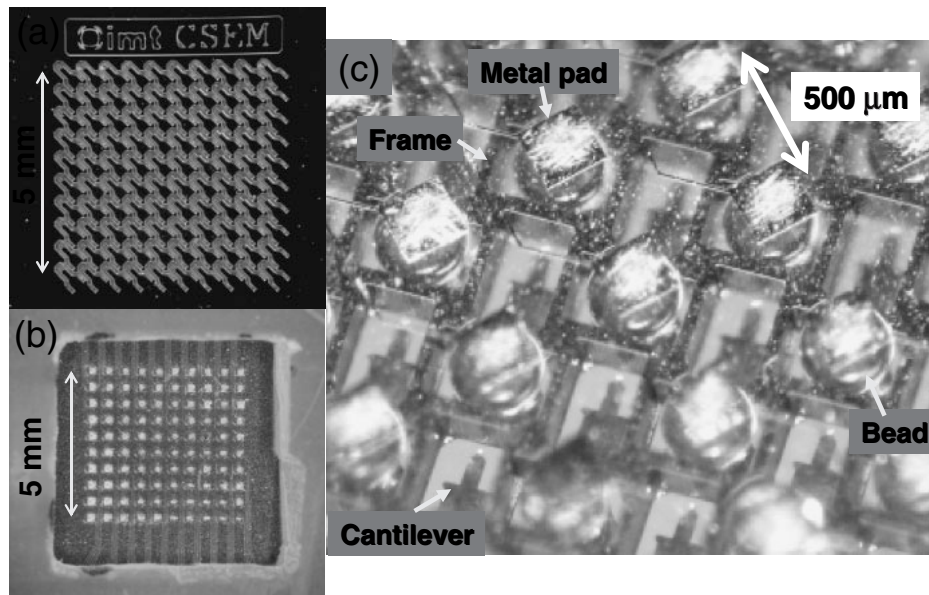


Fig. 5. (a) Top view of  $10 \times 10$  probe array, (b) view from the back surface of the PCB, and (c) enlarged view of the probe array area showing the cantilevers and beads through Mylar film.

Fig. 4(b)]. The required alignment tolerance between the pads on the Mylar film and those on the PCB was about 0.5 mm. Next, the probe array chip was placed on a small metal blanket to hold the chip relative to the PCB in the final assembly. The blanket is not shown in Fig. 4(a), but is shown in Fig. 4(b). The beads were manually dropped into the cavities of the probe array chip with tweezers under an optical microscope. The cavities were well defined by photolithography and DRIE. The beads were automatically positioned within  $10 \mu\text{m}$  accuracy. The PCB with the Mylar film was aligned with the probe array chip and assembled with the metal blanket. Since the probe array chip was tightly fixed between the PCB and the blanket and the beads were covered with the Mylar film to prevent spilling out of the cavities, the handling of this PCB assembly was easy. In this step, only a small surface area on the top of the bead, which is on the central axis of the bead and about  $30 \mu\text{m}$  in diameter, was required to be on the pads with  $250 \mu\text{m}$  square. Manual alignment under optical microscope was sufficient. Figure 5 shows three photographs of the PCB assembly after the array chip was incorporated. Figure 5(a) shows the top view of the probe array. The cantilevers attached to the hinges were designed with a  $45^\circ$  inclination in the  $xy$ -plane in order to have a maximum length within a  $500 \times 500 \mu\text{m}^2$  area. A view from the back surface of the PCB assembly is shown in Fig. 5(b). All pads and lines can be seen. A close up view of the cantilever area is shown in Fig. 5(c). One can see the cantilever with the hinge, the beads, and the chip frame through the Mylar film. The metal pads and interconnections are also seen in this picture. Next, the sliced piezoceramic actuator was fixed on a plane glass plate with conductive epoxy. This unit was attached on the base support with wax, which becomes soft at  $100^\circ\text{C}$  [Fig. 4(c)]. The height position and title of the actuator unit was roughly adjusted while the wax was softened. In the final step, the PCB assembly was incorporated with the base support such that the hinges of the probe array were all pushed up slightly by the piezoceramic blocks. The adjust-

ment of the relative height and title of the PCB assembly against the piezoceramic actuator was carried out by tuning the gaps between the PCB assembly and the base support at four corners. The alignment criterion in the parallel plane was that the small surface area of the bead had to be on the piezoceramic actuator with a  $300 \mu\text{m}^2$  top surface. This step was also manually carried out.

### 3. Characterization

During the assembly of the demonstrator, we found that all cantilevers could not be equally pushed up. The cantilevers at the periphery of the array were pushed up too much, whereas the ones in the center were not pushed up enough. The reason for this was a deformation in the frame of the probe array chip due to insufficient mechanical strength. Nonetheless, we measured the displacements of the cantilevers. A triangular wave was simultaneously applied to all the piezoceramic actuation sections. The displacement yielded at the free end of each cantilever was optically measured. Figure 6 shows a typical displacement of a single cantilever as a function of time. The black line shows the measurement and the blue dotted line shows the driving triangular wave. A displacement of a  $1.6 \mu\text{m}$  peak to peak was obtained with a  $\pm 168 \text{V}_{\text{p-p}}$  driving signal at 0.5 Hz. The output displacement slightly deviated from a straight line, which is most likely due to the property of the piezoceramic block, i.e., hysteresis. The mechanical amplification by the elastic hinge was about 3. Figure 7 shows the measurements of the one hundred cantilevers operated with  $\pm 168 \text{V}_{\text{p-p}}$  driving voltage at 1 Hz. It can be seen that the displacement of the cantilever is larger at the periphery of the array than at the center. A preloading force on the hinge of 50–70 mN per probe has been estimated from the initial assembly condition. The obtained maximum actuation of a single probe was  $2.19 \mu\text{m}_{\text{p-p}}$  ( $6.5 \text{nm/V}$ ). During the experiment, we found that not only the cantilevers but also the array chip itself was slightly being moved up and down, by roughly  $150 \text{nm}_{\text{p-p}}$ , under the circumstance that the one hundred

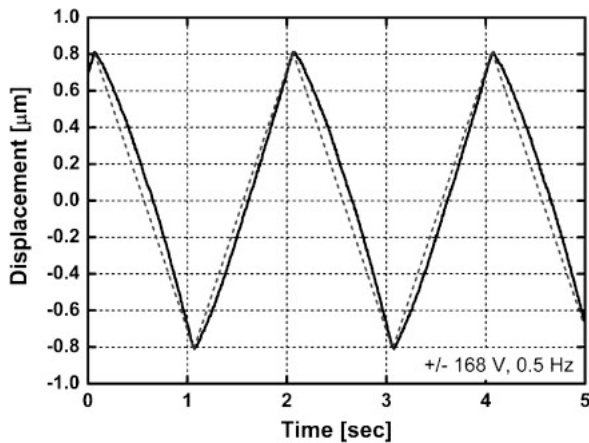


Fig. 6. Displacement of single cantilever.

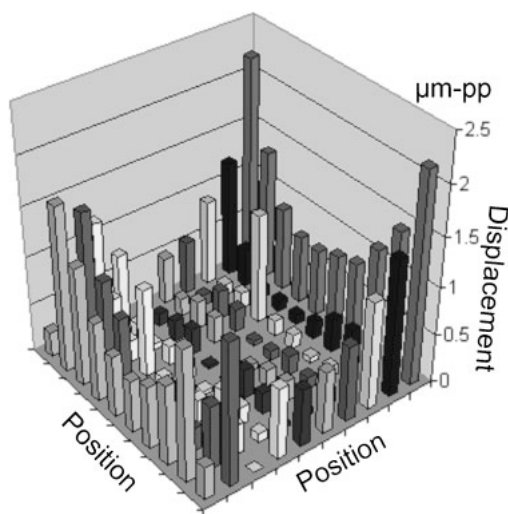


Fig. 7. Displacements of one hundred cantilevers in array.

cantilevers are simultaneously operated. When half of the cantilevers were activated, a mechanical crosstalk on the cantilevers that were not actuated was observed.

#### 4. Conclusions

A concept of an array actuator that is placed outside the

probe chip and used for controlling the tip-sample separation of cantilevers in a probe array AFM system, was proposed and the feasibility of the concept was demonstrated. A  $10 \times 10$  array actuator with  $500 \mu\text{m}$  pitch was made by slicing a bulk piezoceramic plate. The obtained maximum actuation of a single probe was  $2.19 \mu\text{m}_{\text{p-p}}$  at  $\pm 168 \text{ V}_{\text{p-p}}$ . A major issue was the insufficient strength of the frame of the probe array chip. The demonstrated array actuator is highly compatible with a targeting probe array AFM system using either a parallel optical beam or integrated piezoresistive deflection sensing.

Further optimization and design fine tuning are required in order to improve uniformity, mechanical stability and crosstalk. Of course, materials with a higher actuation efficiency than PZT are also very desirable. The external actuation concept has great potential for non-disposable and inexpensive probe array actuation.

#### Acknowledgments

This project was financed by the Board of the Swiss Federal Institutes of Technology through the program TOPNANO21. We thank the technical staff of the CSEM/IMT common lab COMLAB for their support.

- 1) S. C. Minne, J. D. Adams, G. Yaralioglu, S. R. Manalis, A. Atalar, and C. F. Quate: *Appl. Phys. Lett.* **73** (1998) 1742.
- 2) P. Vettiger, G. Cross, M. Despont, U. Drechsler, U. Durig, B. Gotsmann, W. Haberle, M. A. Lantz, H. E. Rothuizen, R. Stutz, and G. K. Binnig: *IEEE Trans. Nanotechnol.* **1** (2002) 39.
- 3) T. Akiyama, U. Staufer, N. F. de Rooij, D. Lange, C. Hagleitner, O. Brand, H. Baltes, A. Tonin, and H. R. Hidber: *J. Vac. Sci. Technol. B* **18** (2000) 2669.
- 4) L. Aeschimann, F. Goericke, J. Polesel Maris, A. Meister, T. Akiyama, B. Chui, U. Staufer, R. Pugin, H. Heinzelmann, N. F. de Rooij, W. P. King, and P. Vettiger: *Int. Conf. Nanoscience and Technology (ICN+T)*, Basel, Switzerland, 2006, No. 87.
- 5) J. Polesel-Maris, L. Aeschimann, A. Meister, R. Ischer, E. Bernard, T. Akiyama, M. Giazzon, P. Niedermann, U. Staufer, R. Pugin, H. Heinzelmann, N. F. de Rooij, and P. Vettiger: *Int. Conf. Nanoscience and Technology (ICN+T)*, Basel, Switzerland, 2006, No. 85.
- 6) O. Manzardo, L. Chantada, M.-S. Kim, L. Aeschimann, T. Akiyama, N. F. de Rooij, U. Staufer, P. Vettiger, R. Dandliker, and H. Herzig: *Int. Conf. Nanoscience and Technology (ICN+T)*, Basel, Switzerland, 2006, No. 86.
- 7) M.-S. Kim, O. Manzardo, R. Dandliker, and H. P. Herzig: *Proc. MOEMS 2005*, 2005, p. 173.